THE BULLETIN OF OKAYAMA UNIVERSITY OF SCIENCE No. 40 A pp. 21-30(2004)

K^0 photoproduction on the deuteron

Agus SALAM and Kazuya MIYAGAWA

Simulation Science Center,
Okayama University of Science,
Ridai-cho 1-1, Okayama 700-0005, Japan

(Received September 28, 2004; accepted November 5, 2004)

The K^0 photoproduction on the deuteron is analyzed by investigating the effects of the hyperon-nucleon and the kaon-nucleon rescattering in the final state and the pion mediated process $\gamma d \to \pi NN \to KYN$. A remarkable effect of the hyperon-nucleon rescattering is found in the threshold region of the inclusive cross section. The effect of the pion mediated process is significant for the kaon at a larger kaon scattering angles with smaller momenta, whereas the kaon-nucleon rescattering is much less important. Besides the cross sections, polarization observables are also studied with respect to the final states interactions. The extraction of the elementary amplitudes is shown in the frame work of the impulse approximation.

1 Introduction

The study of the kaon photoproduction has drawn attention for more than three decades since the work of Thom [1]. The advent of a new generation of high duty-factor accelerators with sufficiently high energy such as ELSA in Bonn or CEBAF in Newport News has triggered several new analyses [2-6]. These analyses investigated the proton channels $\gamma p \to K^+\Lambda$ and $\gamma p \to K^+\Sigma^0$ since a large number of experimental data have become available for these channels [7, 8]. Free neutron targets are not available for the study of the neutron channels because of their short lifetime. Instead one uses light nuclei like deuteron which has small binding energy and simple structure as effective neutron targets. With the purpose to extract the elementary cross section on a neutron target, Li *et al.* [9] have calculated the reactions $\gamma d \to K^0\Lambda p$, $\gamma d \to K^0\Sigma^0 p$, and $\gamma d \to K^+\Sigma^- p$ in the impulse approximation (IA) only. They concluded that the deuteron can be used to study K^0 and K^+ photoproduction on the neutron. The study of the hyperon-nucleon interaction is another important aspect of kaon photoproduction on the deuteron. Several investigations of this issue exist already. Renard and Renard [10, 11] have derived the formalism and studied the Λn interaction in kaon photoproduction on the deuteron. Adelseck and Wright [12] have examined the Λn final state interaction in kaon photoproduction from the deuteron via a distorted wave formalism by using a simple Λn potential. With the intention of investigating the hyperon-nucleon (YN) interaction, in a recent paper Yamamura *et al.* [13] have calculated YN final state interaction for the K^+ channels by using the more realistic Nijmegen YN potentials [14, 15]. They found sizeable effects of the YN interaction in both exclusive and inclusive cross sections, in particular a cusplike structure near the Σ-threshold. Also they concluded that precise data would allow to study the YN interaction in greater detail. This work is extended in the work of A. Salam [16] by including the contribution from kaon-nucleon (KN) rescattering in the final state and pion mediated process $\gamma d \to \pi NN \to KYN$ (πK-process for short) in the intermediate state of the reaction. Another recent calculation is by Kerbikov [17] which also investigated YN final state interaction. A very recent study of two-body contributions to the photoproduction operator was published by Maxwell [18] using a diagrammatic approach where the pion mediated process is included in lowest order but without YN and KN rescattering.

In the present paper, we extend the work of Yamamura *et al.* [13] by calculating the K^0 photoproduction on the deuteron and taking into account the effects of KN rescattering and πK-process. Special attention is paid for the channel $\gamma d \to K^0\Lambda p$ in order to show the possibility of extracting the invariant elementary amplitude from the cross section. In Sect. 2, we briefly review the production operator used in this work. The formalism of calculating the transition matrix and the cross section for kaon photoproduction on the deuteron is shown in Sect. 3. The results are presented in Sect. 4 and we close the paper with some conclusions in Sect. 5. Throughout the paper we use the natural units $\hbar = c = 1$.

2 The kaon photoproduction operator

Almost all analyses of kaon photoproduction on the nucleon were performed at tree level [2-6] in an effective Lagrangian approach. While this leads to the violation of unitarity, this kind of isobaric model provides a simple tool to parametrize kaon photoproduction on the nucleon because it is relatively easy to calculate and to use for production on nuclei. In this approach, the photoproduction amplitude has the form

$$\langle \mu_Y | t_\lambda^{\gamma K} | \mu_N \rangle = \bar{u}_{\mu_Y} \Big(\sum_{i=1}^{4} A_i \Gamma_\lambda^i \Big) u_{\mu_N} \, , \quad (2.1)$$

where A_i's are invariant amplitudes as functions of the Mandelstam variables only. The hyperon and nucleon Dirac spinors are denoted by u_{μ_Y} and u_{μ_N}, respectively. The invariant Dirac operators Γ_λ^i, which are given by

$$\begin{aligned} \Gamma_\lambda^1 &= \tfrac{1}{2}\gamma_5 \left(\not\epsilon_\lambda \not k - \not k \not\epsilon_\lambda \right) , & (2.2) \\ \Gamma_\lambda^2 &= \gamma_5 \left[(2q-k)\cdot\epsilon_\lambda P\cdot k \right. \\ & \quad \left. -(2q-k)\cdot k P\cdot\epsilon_\lambda \right] , & (2.3) \\ \Gamma_\lambda^3 &= \gamma_5 \left(q\cdot k \not\epsilon_\lambda - q\cdot\epsilon_\lambda \not k \right) , & (2.4) \\ \Gamma_\lambda^4 &= i\epsilon_{\mu\nu\rho\sigma}\gamma^\mu q^\nu \epsilon_\lambda^\rho k^\sigma , & (2.5) \end{aligned}$$

are gauge invariant Lorentz pseudoscalars. They are given in terms of the usual γ-matrices, the photon momentum k, and its polarization vector ϵ_λ. Here λ labels the polarization states, q is the meson momentum, and $P = (p'+p)/2$, where p and p' denote initial and final baryon momenta, respectively [19]. By expressing the Dirac operators and spinors in term of Pauli matrices $\{1, \vec{\sigma}\}$ and spinors χ, we can write the kaon photoproduction operator as

$$t_\lambda^{\gamma K} = i \left(L_\lambda + i\vec{\sigma}\cdot\vec{K}_\lambda \right) , \quad (2.6)$$

where L_λ and $\vec{K}_\lambda$ are functions of A_i. The rather lengthy expression of A_i, L_λ, and $\vec{K}_\lambda$ can be found in the work of Mart [20].

In the present work we use the model of Mart *et al.* [4] which included the $D_{13}(1900)$ resonance beside the Born terms and other resonances. Separate hadronic form factors for each vertex were used which, however, destroys gauge invariance. In order to restore gauge invariance, a recipe from Haberzettl [21] was utilized. The coupling constants and cut-off parameters were determined by fitting to the experimental data. Fig. 1 shows the total cross section for the various channels as obtained from this model together with experimental data [8]. One readily notes that the model describes the data fairly well.

3 The reaction on the deuteron

The cross section in the deuteron rest frame is given by

$$\begin{aligned} d\sigma &= \frac{1}{6}\sum_\alpha \frac{(2\pi)^3}{4E_\gamma E_K} \frac{d\vec{p}_K}{(2\pi)^3} \frac{d\vec{p}_Y}{(2\pi)^3} \frac{d\vec{p}_N}{(2\pi)^3} \\ &\times \left| \sqrt{2} \langle \Psi^{(-)}_{\mu_Y \mu_N} | t_\lambda^{\gamma K} | \Psi_{\mu_d} \rangle \right|^2 \\ &\times (2\pi)^4 \delta^4 (P_d + Q - p_Y - p_N) , \quad (3.1) \end{aligned}$$

where $\alpha = \{\mu_Y, \mu_N, \mu_d, \lambda\}$ denote the spin projections of hyperon, nucleon, deuteron and the photon polarization, respectively. Here $Q = p_\gamma - p_K$ is the momentum transfer and the factor $\sqrt{2}$ comes from the proper antisymmetrization. In this expression the dependencies on the kinematical variables have been suppressed and it should be understood that the operator $t^{\gamma K}$ acts on one of the two initial baryons. For the inclusive process $d(\gamma, K)YN$ the cross section is given by

$$\begin{aligned} \frac{d\sigma}{dp_K d\Omega_K} &= \frac{1}{6}\sum_\alpha \int d\Omega_Y^{cm} \frac{m_Y m_N |\vec{p}_K|^2 |\vec{p}_Y^{cm}|}{4(2\pi)^2 E_\gamma E_K W} \\ &\times \left| \sqrt{2} \langle \Psi^{(-)}_{\mu_Y \mu_N} | t_\lambda^{\gamma K} | \Psi_{\mu_d} \rangle \right|^2 , \quad (3.2) \end{aligned}$$

where $W^2 = (P_d + Q)^2$ and $|\vec{p}_Y^{cm}|$ is calculated in the center of mass frame of the two final baryons. In arriving at this expression the factor $(m_Y/E_Y)(m_N/E_N) \times (E_Y/m_Y)(E_N/m_N)$ has been inserted in Eq. (3.1). The second factor multiplies the nuclear matrix element which is treated non-relativistically. Thus one can replace it by unity. The detail of these derivations can be found in the work of Yamamura *et al.* [13]. The cross section for the exclusive process $d(\gamma, KY)N$ is given by

$$\begin{aligned} \frac{d\sigma}{dp_K d\Omega_K d\Omega_Y'} &= \frac{1}{6}\sum_\alpha \frac{m_Y m_N |\vec{p}_K|^2 |\vec{p}_Y|^2}{4(2\pi)^2 E_\gamma E_K} \\ &\times \left| E_0 |\vec{p}_Y| - E_Y |\vec{Q}| \cos\theta_Y' \right|^{-1} \\ &\times \left| \sqrt{2} \langle \Psi^{(-)}_{\mu_Y \mu_N} | t_\lambda^{\gamma K} | \Psi_{\mu_d} \rangle \right|^2 , \end{aligned} \quad (3.3)$$

where $E_0 = E_\gamma + m_d - E_K$ and $\vec{Q}$ is the momentum transfer. The angle θ'_Y is measured relative to the direction of $\vec{Q}$.

The amplitude is approximated by the diagram shown in Fig. (2), which is written for convenience as

$$\langle \Psi^{(-)}_{\mu_Y \mu_N} | t^{\gamma K}_\lambda | \Psi_{\mu_d} \rangle \;=\; \langle \mu_Y \mu_N | T^{\gamma K}_\lambda | \Psi_{\mu_d} \rangle \tag{3.4}$$

with

$$T^{\gamma K} \;=\; t^{\gamma K} + t^{\gamma K}_{YN} + t^{\gamma K}_{KN} + t^{\gamma K}_{K\pi}, \tag{3.5}$$

where $t^{\gamma K}$, $t^{\gamma K}_{YN}$, $t^{\gamma K}_{KN}$, and $t^{\gamma K}_{K\pi}$ denote the operators for the impulse approximation, hyperon-nucleon rescattering, kaon-nucleon rescattering, and the pion mediated process, respectively.

The IA and YN rescattering terms are calculated very precisely. Here we describe the calculation briefly. The reader should consult to Ref. [13] for the detail. The operator of diagrams (a) and (b) can be written as

$$T^{\gamma K}_{YN} \;=\; t^{\gamma K} + t^{\gamma K}_{YN} \tag{3.6}$$

$$\;=\; t^{\gamma K} + t_{YN}\, G_{YN} t^{\gamma K} \tag{3.7}$$

with the YN scattering operator t_{YN} which obeys the Lippmann-Schwinger equation

$$t_{YN} \;=\; V_{YN} + V_{YN}\, G_{YN}\, t_{YN}\,, \tag{3.8}$$

where V_{YN} denotes the YN potential operator and G_{YN} the free YN propagator. Inserting Eq. (3.8) in Eq. (3.7), we get

$$T^{\gamma K}_{YN} \;=\; t^{\gamma K} + V_{YN}\, G_{YN}\, T^{\gamma K}_{YN}\,, \tag{3.9}$$

which can be solved by inversion

$$T^{\gamma K}_{YN} \;=\; (1 - V_{YN}\, G_{YN})^{-1}\, t^{\gamma K}\,. \tag{3.10}$$

After solving the last equation in the partial wave decomposition with respect to the YN subsystem, one obtains the YN rescattering amplitude by subtraction of the IA term.

The KN rescattering (diagram (c) of Fig. 2) is evaluated directly in contrast to YN rescattering. The corresponding operator is given by

$$t^{\gamma K}_{KN} \;=\; t_{KN}\, G_{KN}\, t^{\gamma K}\,, \tag{3.11}$$

where t_{KN} is the KN scattering operator, which also obeys the Lippmann-Schwinger equation of the form (3.8), and G_{KN} is the free KN propagator. For V_{KN} we take the rank-1 separable potential which, in the partial wave representation, is given by

$$V_{\ell J}(p', p) \;=\; \lambda_{\ell J}\, g(p')_{\ell J}\, g(p)_{\ell J} \tag{3.12}$$

with the form factor

$$g(p)_{\ell J} \;=\; \frac{B_{\ell J}\, p^\ell}{[p^2 + A^2_{\ell J}]^{\frac{\ell+2}{2}}}\,, \tag{3.13}$$

where $\lambda_{\ell J}$, $B_{\ell J}$, and $A_{\ell J}$ are parameters which are determined by fitting the phaseshift to the experimental data [22, 23]. The πK-process (diagram (d) of Fig. 2) is also calculated in the same way as in the case of KN rescattering. The detail of these calculation can be found in the work of A. Salam [16].

In the following we describe briefly the extraction of the invariant elementary amplitude from the cross section on the deuteron in view of the study of kaon photoproduction on the neutron. Here we consider only the channel $\gamma d \to K^0 \Lambda p$ as its measurement is more realizable in the near future. The condition for extracting is that the final state interaction effects are negligible. In this case one can separate the invariant elementary amplitude from the deuteron one. To show this, first we write the amplitude of the impulse term explicitly as

$$\langle \mu_Y \mu_N | t^{\gamma K}_\lambda | \Psi_{\mu_d} \rangle = \sum_{\mu_{N'}} \langle \mu_Y | t^{\gamma K}_\lambda | \mu_{N'} \rangle \times C^{\frac{1}{2}\frac{1}{2}1}_{\mu_N \mu_{N'} \mu_S}\, \Psi_{\mu_S \mu_d}(-\vec{p}_N)\,, \tag{3.14}$$

where C is Clebsch-Gordan coefficient, $\vec{p}_N$ is the spectator nucleon momentum, and Ψ is the deuteron wave function. This wave function is given by

$$\Psi_{\mu_S \mu_d}(-\vec{p}_N) \;=\; \sum_\ell C^{\ell\, 1\, 1}_{\mu_\ell \mu_S \mu_d}\, u_\ell(|\vec{p}_N|) \times\; Y_{\ell \mu_\ell}(-\hat{p}_N)\,, \tag{3.15}$$

where Y is the spherical harmonics and u is its radial part. We used the Bonn model [24] for generating the deuteron wave function. Then by explicit calculation of summation over all spin state of the amplitude given in Eq. (3.14) finally we get

$$\sum_{\mu_Y \mu_N \mu_d \lambda} \left| \langle \mu_Y \mu_N | t^{\gamma K}_\lambda | \mu_d \rangle \right|^2 = \sum_{\mu_Y \mu_{N'}} \left| \langle \mu_Y | t^{\gamma K}_\lambda | \mu_{N'} \rangle \right|^2 \left[\tfrac{3}{2} |Y_{00}|^2 u_0^2 + \left(\tfrac{3}{10} |Y_{20}|^2 + \tfrac{3}{5} |Y_{21}|^2 + \tfrac{3}{5} |Y_{22}|^2 \right) u_2^2 \right], \tag{3.16}$$

where the first factor on the r.h.s. is the invariant elementary amplitude for the reaction $\gamma N' \to KY$.

4 Results

In Fig. 3 we present the result for the total cross section of $\gamma d \to K^0 \Lambda p$, $\gamma d \to K^0 \Sigma^+ n$, and $\gamma d \to K^0 \Sigma^0 p$, which is obtained by integrating Eq. (3.2) over kaon angles and momenta. As can be seen from the panels in the top row of the figure, the πK-process (solid line) has a remarkable effect especially in Σ-channel. The panels in the bottom row of the figure show the ratio $\sigma^{IA+FSI}/\sigma^{IA}$. From this ratio we can see that the effects of YN rescattering and πK-process are strong near the threshold region. For all channels being considered the effect of KN rescattering is almost negligible.

Fig. 4 shows the differential cross section, which is obtained by integrating Eq. (3.2) over kaon angles, as a function of kaon scattering angle θ_K in the deuteron rest frame (top row panels) and the ratio $d\sigma^{IA+FSI}/d\sigma^{IA}$ (bottom row panels). Here the cross section is calculated at the photon energy near the threshold. Therefore, as it is shown in the top row panels, the πK-process has a remarkable effect. The next strong effect comes from YN rescattering, while KN rescattering again shows a negligible effect. From this figure we can see that the kaon is scattered mostly in the forward direction. This is because the deuteron wave function is suppressed in the backward angle. However the ratio $d\sigma^{IA+FSI}/d\sigma^{IA}$ shows that the rescatterings and πK-process have strong effects at the backward angles. This can be explained that the rescatterings and πK-process have redistributed the relative momentum of the nucleons such that the deuteron wave function has larger values in the backward angle.

The inclusive cross section is shown in Fig. 5. In this figure we add the cross section of all channel being considered. The left panel shows the cross section at a smaller photon energy and the right at a higher photon energy. Both are calculated in the forward kaon angle. We can see that the YN rescattering enhances the cross section at the threshold region and also around the peak for the both photon energies, while the πK-process shows its effect at smaller kaon momentum and photon energy. Fig. 6 shows the inclusive cross section only with IA which is calculated using two different elementary operators. The solid one is calculated using elementary operator with $D_{13}(1900)$ resonance while the dash is without. Here we can see a big difference between those cross sections especially in the Λ-channel. Thus this channel can serve as a filter for the different elementary operators.

In Fig. 7 we present the exclusive cross section calculated for photon energy of 1.3 GeV in the forward kaon angle θ_K at the peak position. The figure shows that the YN rescattering dominates the effect in this region at larger hyperon angle θ'_Y, while KN rescattering and πK-process have negligible effects over all hyperon angle θ'_Y.

The tensor asymmetry is shown in Fig. 8. From this figure we can see that the rescatterings and πK-process have very different effects for T_{20}, T_{21}, and T_{22}, especially at larger kaon scattering angle θ_K. Fig. 9 shows the double polarization observables calculated for photon energies near the threshold in forward angle θ_K, while Fig. 10 the recoil polarization and beam asymmetry. The figures show that the YN rescattering dominates the effect for those polarization observables. The effect is remarkable at larger hyperon angle θ'_Y.

Fig. 11 presents the invariant elementary amplitudes for the channel $\gamma d \to K^0 \Lambda p$. The amplitudes are calculated for photon energy of 1.5 GeV, $\theta_N = 30$ degree, and $\phi_N = 180$ degree. These kinematics are chosen in accordance with the work of Li *et al.* [9]. The left panel shows the amplitudes for $|\vec{p}_N| = 50$ MeV and the right for $|\vec{p}_N| = 500$ MeV. As can be seen, the extracted elementary amplitude is coinside with the free case for the smaller spectator nucleon momentum.

5 Conclusions

We have evaluated the K^0 photoproduction on the deuteron by investigating the effect of YN and KN rescattering and πK-process. A sizeable effect in the total cross section is found from πK-process especially in Σ-channel. The YN rescattering has a remarkable effect at the threshold region in the inclusive cross section, while πK-process has strong effects at the backward kaon angles and for small kaon momentum. In the exclusive cross section the YN rescattering dominates the effect at larger hyperon angles. In all cases the effect of KN rescattering is negligible. It is also found that Λ channel shows very different strength in the inclusive cross section for different elementary operators, which indicates that this channel can serve as a filter for different model of elementary operators. For the polarization observables the YN rescattering has dominant effects than KN rescattering and πK-process.

We also have shown how to extract the elementary amplitude from the cross section on the deuteron for the channel $\gamma d \to K^0 \Lambda p$. It is found that the extracted elementary amplitude is coinside with the free case at a small spectator nucleon momentum, while the discrepancy appears in the larger momentum.

Acknowledgement

AS would like to thank the Simulation Science Center, Okayama University of Science, Okayama for the financial support and for the very kind hospitality during his stay.

References

[1] H. Thom, Phys. Rev. **151**, 1322 (1966).

[2] J.C. David, C. Fayard, G.H. Lamot, and B. Saghai, Phys. Rev. C **53**, 2613 (1996).

[3] C. Bennhold, T. Mart, and D. Kusno, in *Proceedings of the CEBAF/INT Workshop on N* Physics*, Seattle USA, 1996.

[4] T. Mart and C. Bennhold, Phys. Rev. C **61**, 012201 (2000); T. Mart, *ibid.* **62**, 038201 (2000).

[5] B.S. Han, M.K. Cheoun, K.S. Kim, and I.T. Cheon, Nucl. Phys. **A691**, 713 (2001).

[6] S. Janssen, J. Ryckebusch, D. Debruyne, and T.V. Cauteren, Phys. Rev. C **65**, 015201 (2002).

[7] M. Bockhorst *et al.*, Z. Phys. C **63**, 37 (1994).

[8] M.Q. Tran *et al.*, Phys. Lett. **B445**, 20 (1998).

[9] X. Li, L.E. Wright, and C. Bennhold, Phys. Rev. C **45**, 2011 (1992).

[10] F.M. Renard and Y. Renard, Nucl. Phys. **B1**, 389 (1967).

[11] F.M. Renard and Y. Renard, Phys. Lett. **B24**, 159 (1967).

[12] R.A. Adelseck and L.E. Wright, Phys. Rev. C **39**, 580 (1989).

[13] H. Yamamura, K. Miyagawa, T. Mart, C. Bennhold, W. Glöckle, and H. Haberzettl, Phys. Rev. C **61**, 014001 (1999).

[14] P.M.M. Maessen, Th.A. Rijken, and J.J. de Swart, Phys. Rev. C **40**, 2226 (1989).

[15] Th.A. Rijken, V.G.J. Stoks, and Y. Yamamoto, Phys. Rev. C **59**, 21 (1999).

[16] A. Salam, Dissertation, Johannes Gutenberg Universität, Mainz, 2003.

[17] B.O. Kerbikov, Phys. Atom. Nucl. **64**, 1835 (2001).

[18] O.V. Maxwell, Phys. Rev. C **69**, 034605 (2004).

[19] A. Donnachie, *High Energy Physics*, Vol. 5, Academic Press, New York, 1972.

[20] T. Mart, Dissertation, Johannes Gutenberg Universität, Mainz, 1996.

[21] H. Haberzettl, Phys. Rev. C **56**, 2041 (1997); H. Haberzettl, C. Bennhold, T. Mart, and T. Feuster, *ibid.* **58**, R40 (1998).

[22] J.S. Hyslop, R.A. Arndt, L.D. Roper, and R.L. Workman, Phys. Rev. D **46**, 961 (1992).

[23] D.H. Saxon *et al.*, Nucl. Phys. **B162**, 522 (1980).

[24] R. Machleidt, K. Holinde, and Ch. Elster, Phys. Rep. **149**, 1 (1987).

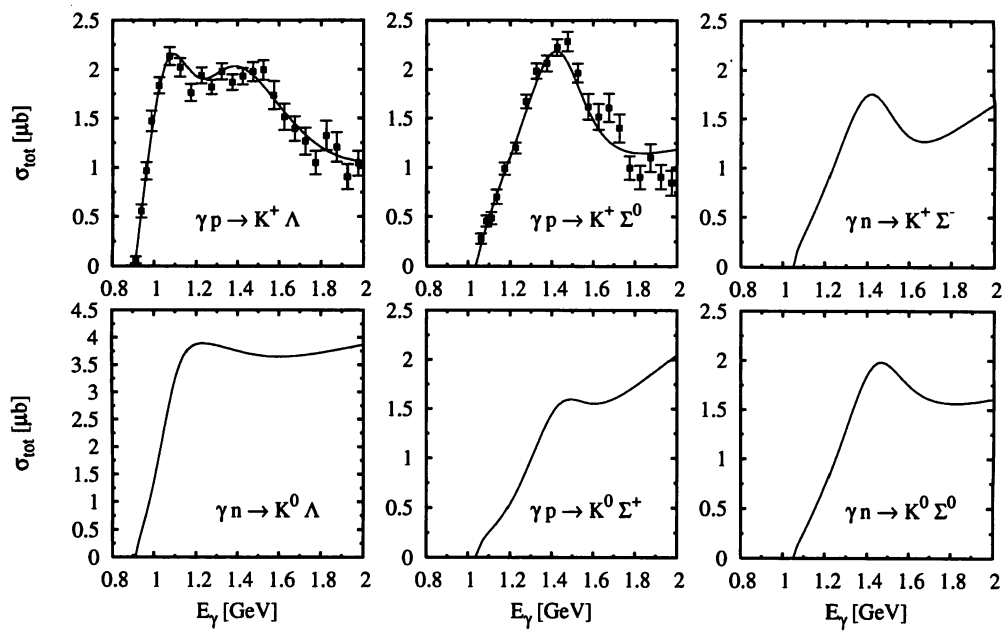

Figure 1: Total cross section of kaon photoproduction on the nucleon using the model of Mart *et al.* [4]. The data are taken from Ref. [8].

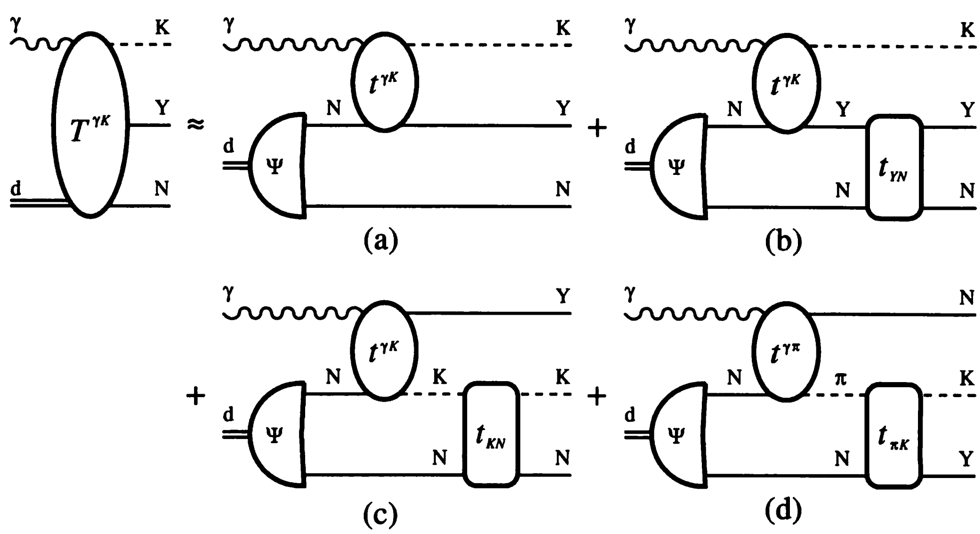

Figure 2: Kaon photoproduction on the deuteron. Diagram (a) is impulse approximation (IA), (b) and (c) are YN and KN rescattering, respectively, and (d) is πK-process.

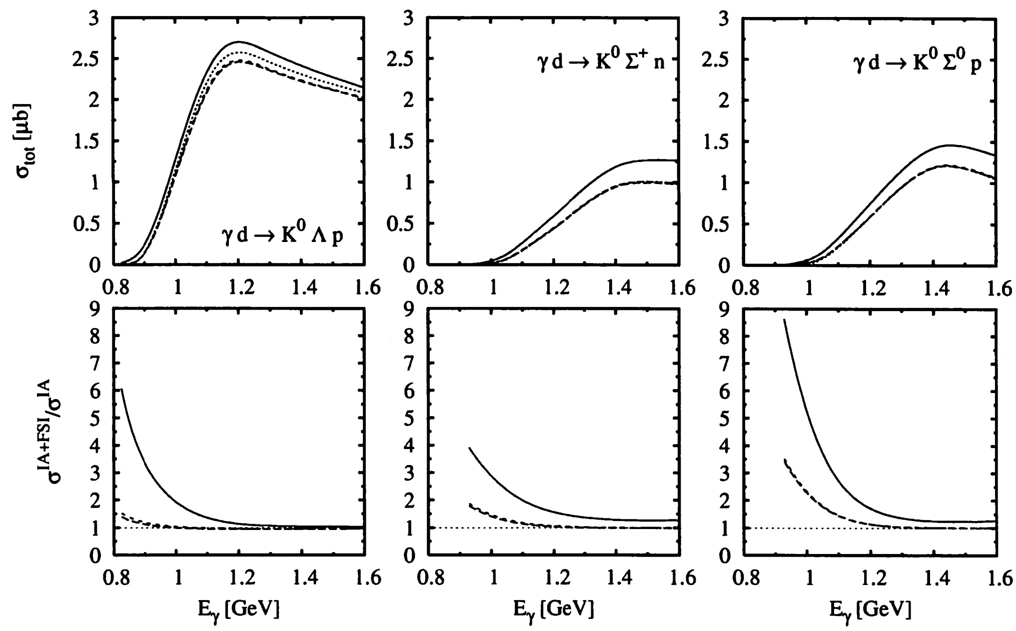

Figure 3: The top row is the total cross section and the bottom the ratio $\sigma^{IA+FSI}/\sigma^{IA}$. The dotted line is the impulse approximation, the short-dash is after included YN rescattering, the dash is KN rescattering, and the solid is the pion mediated process.

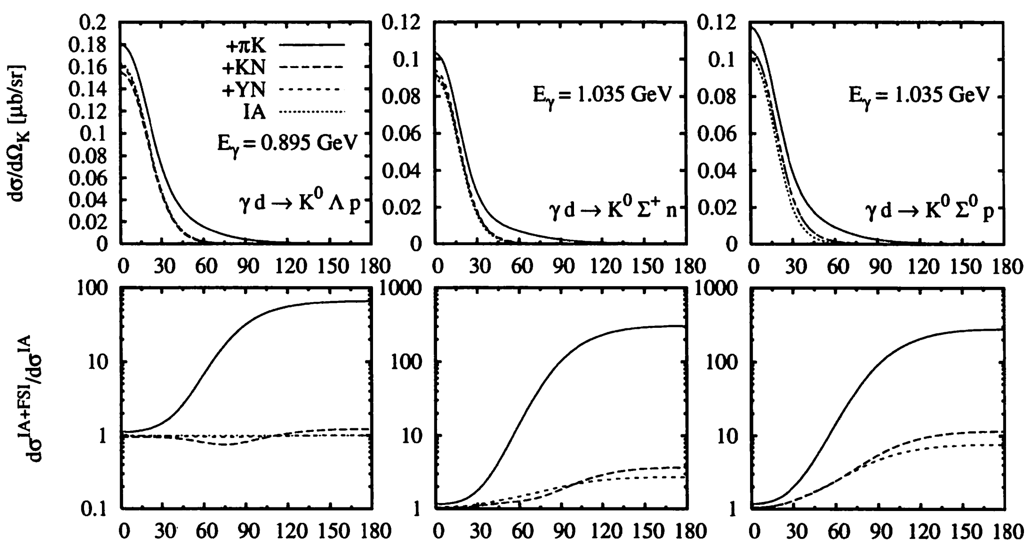

Figure 4: The top row is the differential cross section as a function of θ_K and the bottom the ratio $d\sigma^{IA+FSI}/d\sigma^{IA}$. The notation is the same as the previous figure.

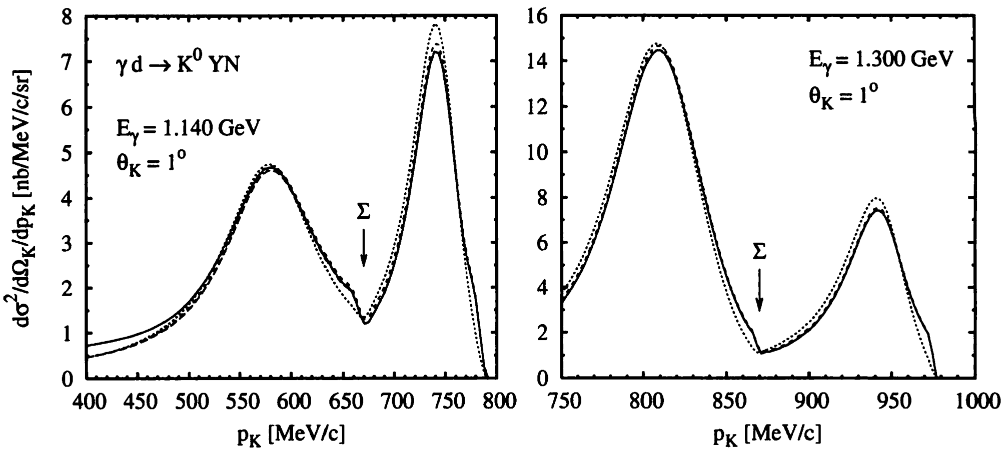

Figure 5: The inclusive cross section at forward θ_K. The left panel is for photon energy of 1.14 GeV and the right of 1.3 GeV. The notation is the same as the previous figure.

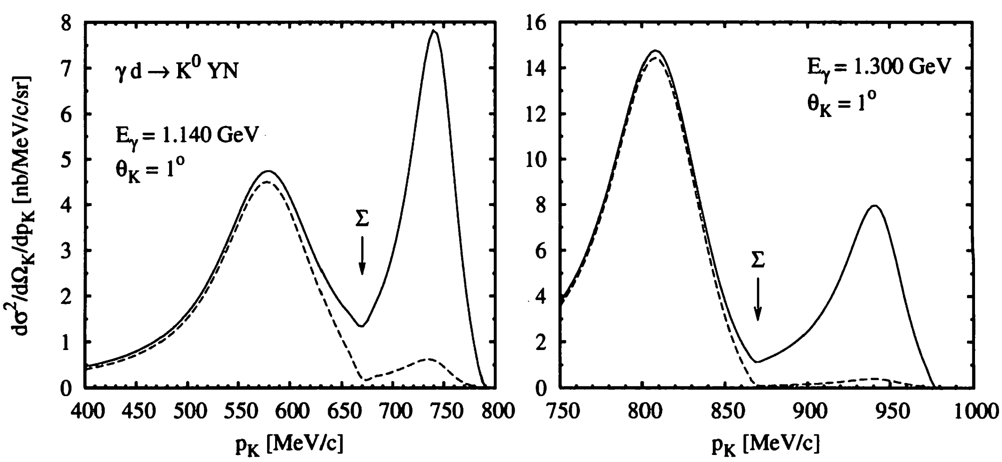

Figure 6: The inclusive cross section only with IA at forward θ_K. The left panel is for photon energy of 1.14 GeV and the right of 1.3 GeV. The solid line is calculated with $D_{13}(1900)$ resonance while the dashed line is without.

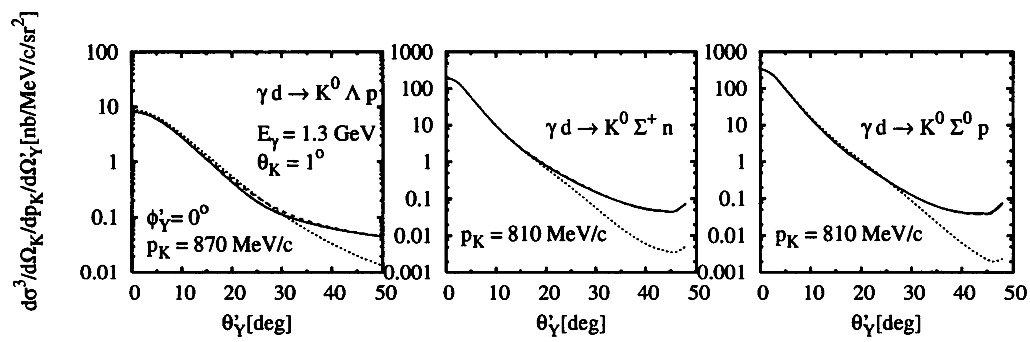

Figure 7: The exclusive cross section for photon energy of 1.3 GeV in the forward θ_K at p_K of 870 MeV/c and 810 MeV/c. The notation is the same as Fig. 5.

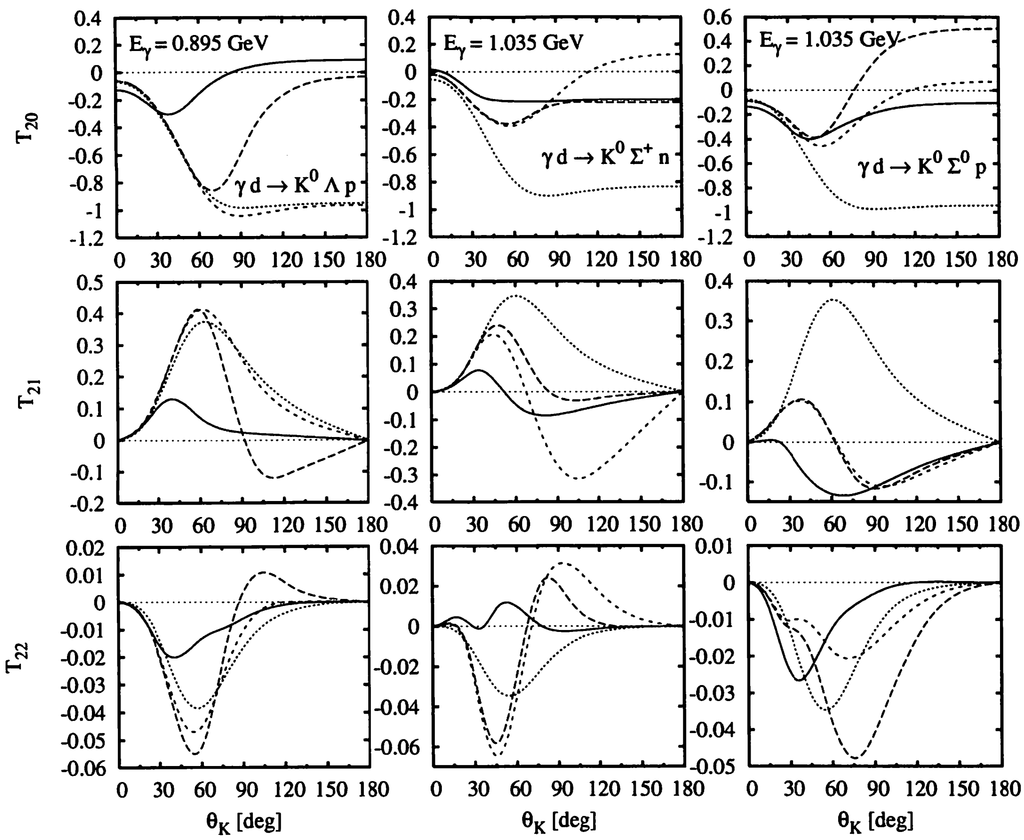

Figure 8: Tensor asymmetry calculated for photon energies near the threshold. The notation is the same as the previous figure.

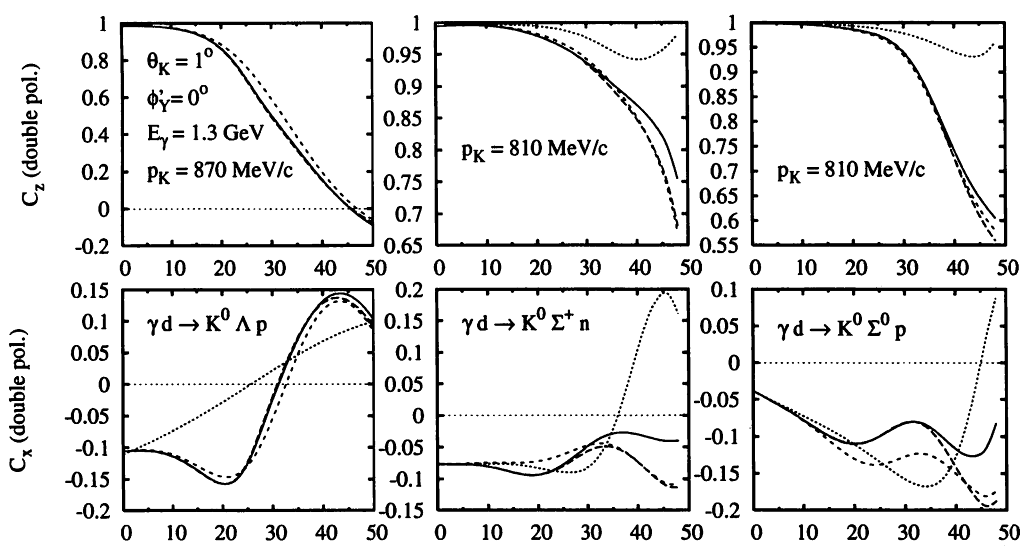

Figure 9: Double polarization observables. The notation is the same as the previous figure.

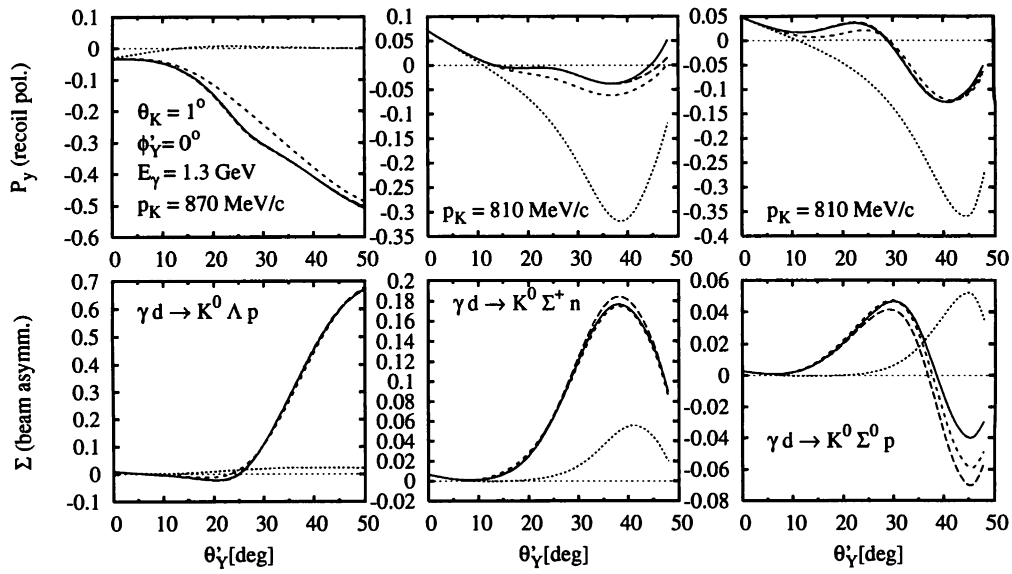

Figure 10: Top panels show the recoil polarization and bottom panels the beam asymmetry. The notation is the same as the previous figure.

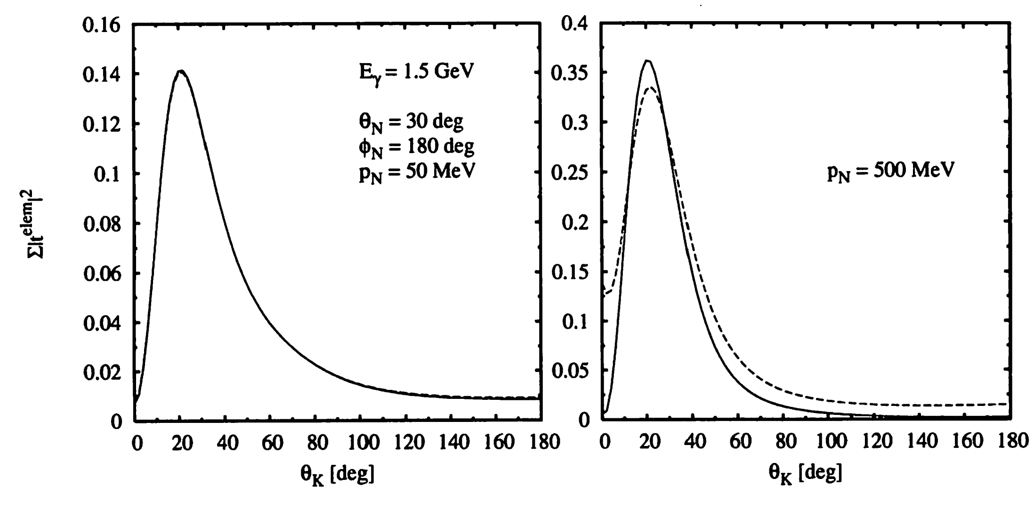

Figure 11: Invariant elementary amplitude for $\gamma d \to K^0 \Lambda p$. The solid line is calculated in the free case while the dash line is extracted from the cross section on the deuteron.